ACS APPLIED MATERIALS & INTERFACES

Research Article

www.acsami.org

Tunable Mechanics in Electrospun Composites via Hierarchical Organization

Nandula D. Wanasekara, Lindsay E. Matolyak, and LaShanda T. J. Korley*

Department of Macromolecular Science and Engineering, Case Western Reserve University, Cleveland, Ohio 44106, United States

Supporting Information

ABSTRACT: Design strategies from nature provide vital clues for the development of synthetic materials with tunable mechanical properties. Employing the concept of hierarchy and controlled percolation, a new class of polymer nanocomposites containing a montmorillonite (MMT)-reinforced electrospun poly(vinyl alcohol) (PVA) filler embedded within a polymeric matrix of either poly(vinyl acetate) (PVAc) or ethylene oxide−epichlorohydrin copolymer (EO−EPI) were developed to achieve a tunable mechanical response upon exposure to specific stimuli. Mechanical response and switching times upon hydration were shown to be dependent on the weight-fraction of MMT in the PVA electrospun fibers and type of composite matrix. PVA/MMT.PVAc composite films retained excellent two-way switchability for all MMT fractions; however, the switching time upon hydration was decreased dramatically as the MMT content was increased due to the highly hydrophilic nature of MMT. Additionally, for the first time, significant two-way switchability of PVA/MMT.EO-EPI composites was achieved for higher weight fractions (12 wt %) of MMT. An extensive investigation into the effects of fiber diameter, crystallinity, and MMT content revealed that inherent rigidity of MMT platelets plays an important role in controlling the mechanical response of these hierarchical electrospun composites.

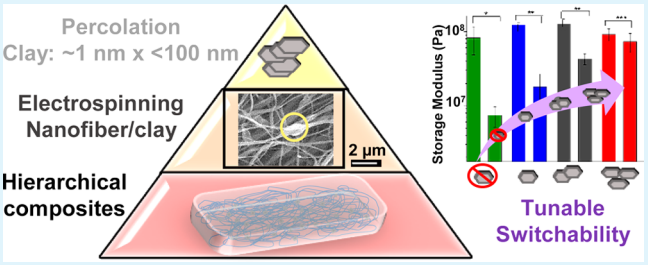

KEYWORDS: *electrospinning, hierarchical composites, stimuli-responsive, tunable mechanics, percolation*

1. INTRODUCTION

Nature utilizes an array of design strategies for engineering materials with multiple and tunable functionalities. These strategies include precise control of hierarchical structure, selective reinforcement of certain domains, and structural and mechanical heterogeneity as a result of spatial distributions in the shape, size, and chemical composition of constituent building blocks.[1] For example, bone consists of a complex hierarchical structure with mineralized collagen platelets reinforcing the collagen fibrils embedded within the extracellular matrix.[2] One strategy inspired by nature for designing mechanically adaptable materials is the utilization of composites in which responsive fibrous and/or particulate fillers are embedded in a matrix material. Critical to the responsive mechanics and the deformation behavior of these composites are the tailored interfacial adhesion and controlled dispersion via percolated networks or self-assembly of filler components. These bioderived strategies, outlined in a recent perspective article,[3] have attracted much attention in the design of stimuli-responsive polymer nanocomposites as highlighted.[4] A relatively unexplored area of research related to bioinspired composites is the incorporation of composite fibers into polymeric matrices as an additional strategy for mechanical tunability.

Several material choices exist for nanofillers in the design and fabrication of polymer nanocomposites. Synthetic layered silicates have been pursued as reinforcing elements in polymer matrices due to their ability to disperse into individual clay layers and their tunable surface chemistry.[5,6] Montmorillonite (MMT) and Laponite are the most widely used layered silicates due to their high aspect ratios and high surface area per mass.[7] The polymer/silicate nanocomposites exhibited notable improvements in material properties, such as stiffness, strength, flammability, and reduced gas permeability.[7−9] Nylon-6/silicate nanocomposites prepared by in situ polymerization of ε-caprolactam exhibited enhanced tensile strength and modulus due to exfoliated silica layers and the formation of hydrogen bonds between silicate layers and the polymer matrix.[10] In other studies,[11,12] hierarchically designed polyurethane composites were fabricated through preferential reinforcement of specific domains of segmented copolymers with an inorganic, unmodified nanoclay filler (Laponite). It was observed that the Laponite layers were favorably attracted to the hydrophilic, continuous soft domain in polyurethanes with hydrophobic hard blocks, and these materials exhibited a microphase-separated morphology but exhibited limited extensibility due to inhibition of strain-induced soft segment alignment.[11] In contrast, the silicate platelets in segmented polyurethanes having both hydrophobic hard and soft domains were preferentially associated within the hard domain, enhancing

Received: July 10, 2015
Accepted: September 21, 2015
Published: October 6, 2015

DOI: 10.1021/acsami.5b06230
ACS Appl. Mater. Interfaces 2015, 7, 22970−22979

the toughness and elastic modulus while preserving the extensibility of the materials.[12] Along with films of clay−polymer composites, fiber clay−polymer composites have also been achieved via electrospinning. Nepalli et al. manufactured hybrid electrospun poly(vinylidene fluoride) fibers with varying weight fractions of MMT, which resulted in improvements of electrospinning mat quality and allowed for the design of structure and morphology that could ultimately control functionality.[13] These studies highlight the ability to tune material properties in hybrid composites via rational control of specific interactions and filler assembly.

Although electrospun nanofibers have been widely used in applications ranging from tissue engineering to filtration, limited studies—mainly in the area of dental resins—have focused on their use as nanofillers in a polymer matrix.[14−17] With a focus on advancements in polymer nanocomposite fabrication, Causin et al. utilized nanofillers of electrospun Nylon-6 to reinforce a poly(ε-caprolactone) matrix, highlighting the simplicity of composite fabrication, the ability to enhance modulus and extensibility synergistically, and the influence on matrix crystallization.[18] Recently, we developed a series of responsive composite systems with electrospun fibers as the filler, exhibiting tunable matrix−filler interactions and responsive mechanics upon hydration.[19,20] In this investigation, by expanding the influence of scale, we have added an additional level of complexity via the incorporation of inorganic MMT into PVA electrospun nanofibers, which were embedded within a rubbery ethylene oxide-*co*-epichlorohydrin (EO-EPI) or poly(vinyl acetate) (PVAc) matrix. PVAc was introduced as a matrix polymer to enhance the stiffness contrast between hard and soft states and for its biocompatibility. EO-EPI was used as the matrix due to its low storage modulus and hydrogen bond accepting nature of the ether functionality of the copolymer. Therefore, a strong interaction between the −OH groups of the PVA filler and the EO-EPI is expected.[4] The dispersion of MMT platelets within the fibers contributes to the first level of hierarchy, and the randomly oriented PVA fibers embedded within the polymeric matrix create the second level. These nanoclay-reinforced hierarchical electrospun composites were investigated with a focus on mechanical switchability and tunability via multicomponent interactions. We have explored the effect of selective reinforcement of a nanofiber filler in a polymer matrix and the role of MMT in mediating matrix−filler interactions on responsive mechanics and filler crystallinity in these hierarchical electrospun composites.

2. EXPERIMENTAL SECTION

2.1. Materials. EO-EPI, trade name Epichlomer C, was purchased from Daiso as a 1:1 comonomer ratio with a density of 1.39 g/mL. Sodium-exchanged montmorillonite (MMT) with a cation exchange capacity (CEC) of 145 mequiv/100 g was purchased from Nanocor Corporation. All other chemicals were purchased from Sigma-Aldrich. Polymer composite matrices were created from either 1:1 EO-EPI (molecular weight, MW ≈ 1000 kg/mol, density = 1.39 g/cm^3) or PVAc (MW ≈ 113 kg/mol, density = 1.19 g/cm^3) and electrospun PVA (MW ≈ 85 kg/mol)/MMT mat filler.

2.2. Methods. To fabricate the electrospun PVA/MMT filler, we created an aqueous solution of PVA (99% hydrolysis)/MMT with varying concentrations of clay (2.5, 7.0, and 12 wt %) as follows. PVA in water was stirred at 80 °C until fully dissolved, and separately, MMT was dissolved in water at room temperature. Once the PVA solution was cooled to room temperature, the two mixtures were added and stirred overnight to produce a homogeneously mixed PVA/MMT solution. The total concentration of PVA in the final solution was 10 (w/v) %, and the MMT concentration (2.5, 7, and 12 wt %) was calculated relative to the PVA weight in the solution. The PVA/MMT solutions were electrospun using a homemade setup described in previous work.[15] Prior to electrospinning, surfactant Triton-X100 was added (1 drop/2.5 mL) to reduce the surface tension of this PVA/MMT solution while stirring for a minimum of 5 min. The PVA/MMT solution with surfactant was then drawn into a syringe using an 18.5 gauge blunt needle, which was loaded onto a pump in the electrospinning apparatus and electrospun under the following conditions: flow rate of 0.8 mL/h, 20 kV, 18 cm tip to rotating collector distance. Larger diameter fibers were spun by decreasing the needle tip-to-collector distance to 10 cm. Once an electrospun mat was formed, it was removed from the collector and immersed in methanol for 24 h. Soaking the mat in methanol prevents dissolution of the fibers in water as a result of increased crystallinity, which also leads to an increase in the storage modulus of the mat.[20] The crystallinity enhancement was attributed to the removal of residual water, which facilitates the replacement of PVA-water hydrogen bonding with intermolecular PVA−PVA hydrogen bonding that act as physical cross-links. Mats were dried under a vacuum for 4 h after the methanol wash and stored in a desiccator.

To fabricate the hierarchical composite, we first solvent cast a polymer matrix, EO-EPI or PVAc, using either toluene or acetone, respectively, into a polytetrafluoroethylene (PTFE) mold and allowed it to dry for 24 h. The PVA/MMT electrospun mat was then placed on top of the matrix film within the PTFE mold, and additional polymer matrix was poured on top of the mat until fully covered. Thus, uniform polymer composites (∼4.0 wt % PVA/MMT filler) were created. Composites using a PVAc matrix were dried for 1 week under ambient conditions followed by 2 weeks at 40 °C under vacuum; this extensive drying process did not impact the PVA crystallinity. PVA/MMT.EO-EPI composites were first dried for 2 days under ambient conditions and then dried further under vacuum for 3 days at room temperature. These thorough drying procedures were carried out to ensure complete removal of casting solvents. In all cases, the electrospun composites were found to be substantially more transparent than the corresponding electrospun mats. Similar transparency levels were observed in electrospun composites fabricated in previous work.[14−17,20−22] This transparency suggests good matrix−filler interactions, which are critical for mechanical reinforcement. For the mechanical and thermal responses of the composites, three stages were examined: dry, initial fabrication state; wet, dry composites exposed to water; and dry-wet-dry, exposed wet composites dried. The wet composites were obtained by soaking in deionized water for 24 h. To obtain the dry-wet-dry composites, wet composites were dried for 24 h under ambient conditions and then further dried under a vacuum at room temperature for 24 h. This intensive drying process was utilized to ensure complete removal of water from the samples and to avoid any effects of plasticization in the dry-wet-dry state. The degree of swelling was determined gravimetrically using eq 1.

$$\text{degree of swelling} = \frac{\text{mass of wet sample} - \text{mass of dry sample}}{\text{mass of dry sample}} \times 100\% \quad (1)$$

Morphological, mechanical, and thermal characterization were performed on neat electrospun mats and the composites. The porosity of the electrospun PVA nanofibers was determined using a Quantachrome Porometer Macro 3G series instrument on a test sample of 1″ diameter. Topographical and cross-sectional morphological characterization was performed using a scanning electron microscope (SEM, JEOL JSM-6510LV), with a chosen voltage of either 25 or 30 kV to obtain optimal SEM images. Prior to performing SEM, the samples were sputter coated with gold (∼9 nm thickness) using a Hummer 6.2 sputtering system with a current of 10 mA. Dispersion of silicate layers within the mats was determined via wide-angle X-ray scattering (WAXS). WAXS data was acquired using an in-house Micromax Rigaku instrument using Cu Kα radiation at a wavelength of 0.1542 nm and collimated using three pinholes. The data were reduced from 2D (intensity vs 2θ, χ) to 1D (intensity vs

DOI: 10.1021/acsami.5b06230
ACS Appl. Mater. Interfaces 2015, 7, 22970−22979

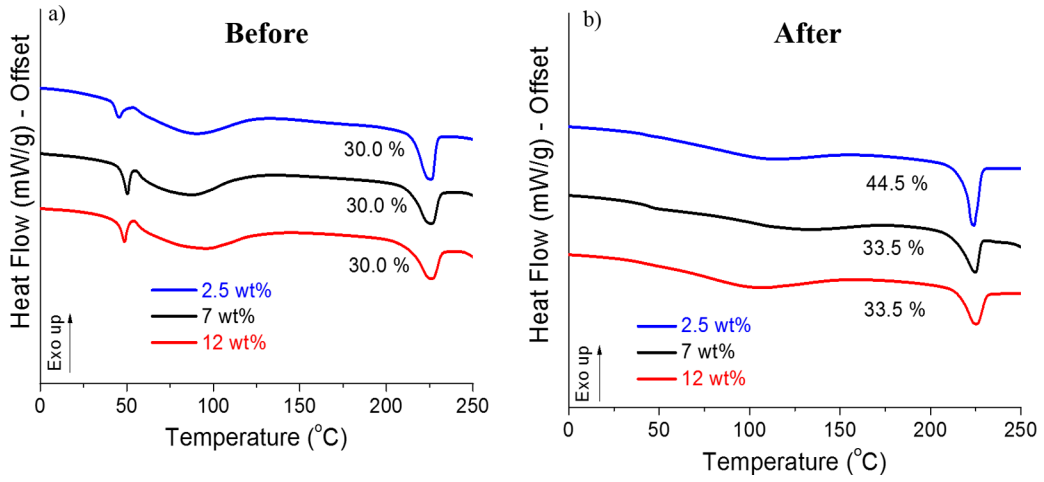

Figure 1. DSC thermograms of PVA electrospun mats as a function of MMT weight fraction (a) before and (b) after methanol treatment.

2θ), where 2θ is the scattering angle and χ is the azimuthal angle. The sample-to-collector distance was calibrated using a silver behenate (AgBe) standard with a 100 scattering vector (q) at a position of 1.076 nm^{-1} to yield a final sample-to-collector distance of 114 mm.

Dynamic and static mechanical characterization were performed utilizing a dynamic mechanical analyzer (DMA) and a tensile tester, respectively. DMA was conducted using a TA Instruments Q800 operating in tensile mode. Testing of the PVA/MMT composites was done at least three times at a frequency of 1 Hz at a constant displacement of 10 μm. The typical samples were rectangular with dimensions of 25 × 3 mm. Hydration-induced storage modulus changes were measured by utilizing a DMA equipped with a submersion chamber (DMA Q800-176). Uniaxial tensile deformation was performed on a Zwick/Roell mechanical testing instrument equipped with a 500 N load cell. Samples were cut according to ASTM D638 with a minimum of three samples for each of the mats and composites. All samples were elongated to failure at a constant strain rate of 100% initial gauge length per minute. Thermal characterization of the PVA/MMT filler-based composites was conducted via thermogravimetric analysis (TGA) and differential scanning calorimetry (DSC). The degradation temperature and the MMT content of the composite films were obtained using TGA (TA Instruments Q500) at a heating rate of 10 °C/min under a nitrogen atmosphere. To examine the thermal behavior (e.g., plasticization and crystallization), we also used a TA Instrument Q100 DSC instrument at a heating rate of 10 °C/min over the temperature range of −90 to 340 °C under a nitrogen atmosphere. The degree of crystallinity was calculated by dividing the melting enthalpy (ΔH) by the enthalpy of melting required for a 100% crystalline PVA sample (ΔH_f = 138.6 J/g).[21]

3. RESULTS AND DISCUSSION

Expanding upon our previous work,[20] an array of hierarchical electrospun composite films was fabricated by varying the matrix polymer (EO-EPI or PVAc) and the MMT content (2.5, 7, and 12 wt %) within the PVA fibers. Unmodified, sodium-exchanged MMT was utilized in this work with strong hydrogen bonding interactions expected between the hydrophilic MMT and PVA. The MMT weight fractions were determined relative to the PVA weight and were chosen to evaluate the role of filler content below and above the percolation threshold of MMT (4 wt %) in PVA.[23] The composite fabrication process produced uniform sandwich structures of films (Figure S1) with an overall PVA/MMT content of 4 wt %. Prior to embedding the mat within the polymeric matrix, the mat was treated with methanol to increase the crystallinity and hydrolytic stability of the PVA/MMT filler. Soaking the PVA fibers in methanol has been shown to enhance the crystallinity.[21] As shown in Figure 1, after the methanol treatment, the PVA mat with 2.5 wt % MMT content exhibited 45% crystallinity, which is similar to that of the neat PVA electrospun mat (46%);[20] however, above the percolation threshold, the 7 and 12 wt % PVA/MMT mats exhibited lower crystallinity values of ∼33.5%. To explore this unexpected phenomenon, we evaluated the initial crystallinity of the as-spun PVA/MMT mats. Interestingly, all the mats exhibited the same degree of crystallinity (∼30%) prior to the methanol soak. There exist several possible scenarios for this observed reduction in crystallinity of PVA/MMT electrospun fibers, particularly above the percolation threshold. One explanation for the lower crystallinity values of methanol-treated PVA/MMT fibers is that, above 4 wt %, the MMT platelets may inhibit the permeation of methanol into the fibers. It has been shown that incorporation of inorganic and/or organic fillers, such as SiO_2[24] and polyrotaxane,[25] into PVA films resulted in a decrease of methanol permeability, which was attributed to the layered structure and high aspect ratios of platelets creating a torturous path for methanol diffusion.[26,27] This reduction in crystallinity of PVA/MMT fibers may be illustrated by examining mathematical models that predict the barrier properties of polymer nanocomposites, which provide insight into the permeability of methanol in PVA. These models propose that the permeability of small molecules, such as methanol, into a polymer matrix is governed by the diffusivity of the small molecule and the total travel path length and sample thickness.[28] In general, the addition of inorganic fillers, such as MMT, could affect the diffusivity in the vicinity of the filler, hindering methanol-directed crystallization of PVA. Another explanation of the reduced crystallinity of PVA/MMT fibers could be rationalized by examining the mechanism driving the enhancement of crystallinity of PVA fibers (without MMT) upon methanol treatment. When the neat PVA fibers are soaked in methanol, any residual water within the fibers is forced out, and the PVA−water hydrogen bonds are replaced by intermolecular PVA−PVA hydrogen bonds, thus increasing the crystallinity. Likewise, the loss of absorbed free water is also exhibited in the DSC curves with the peak at 50 °C disappearing after methanol treatment.[29,30] However, when MMT platelets are incorporated into the fiber, PVA−MMT hydrogen bonds are formed at multiple binding points on the surfaces of MMT platelets;[31] therefore, the formation of new

DOI: 10.1021/acsami.5b06230
ACS Appl. Mater. Interfaces 2015, 7, 22970−22979

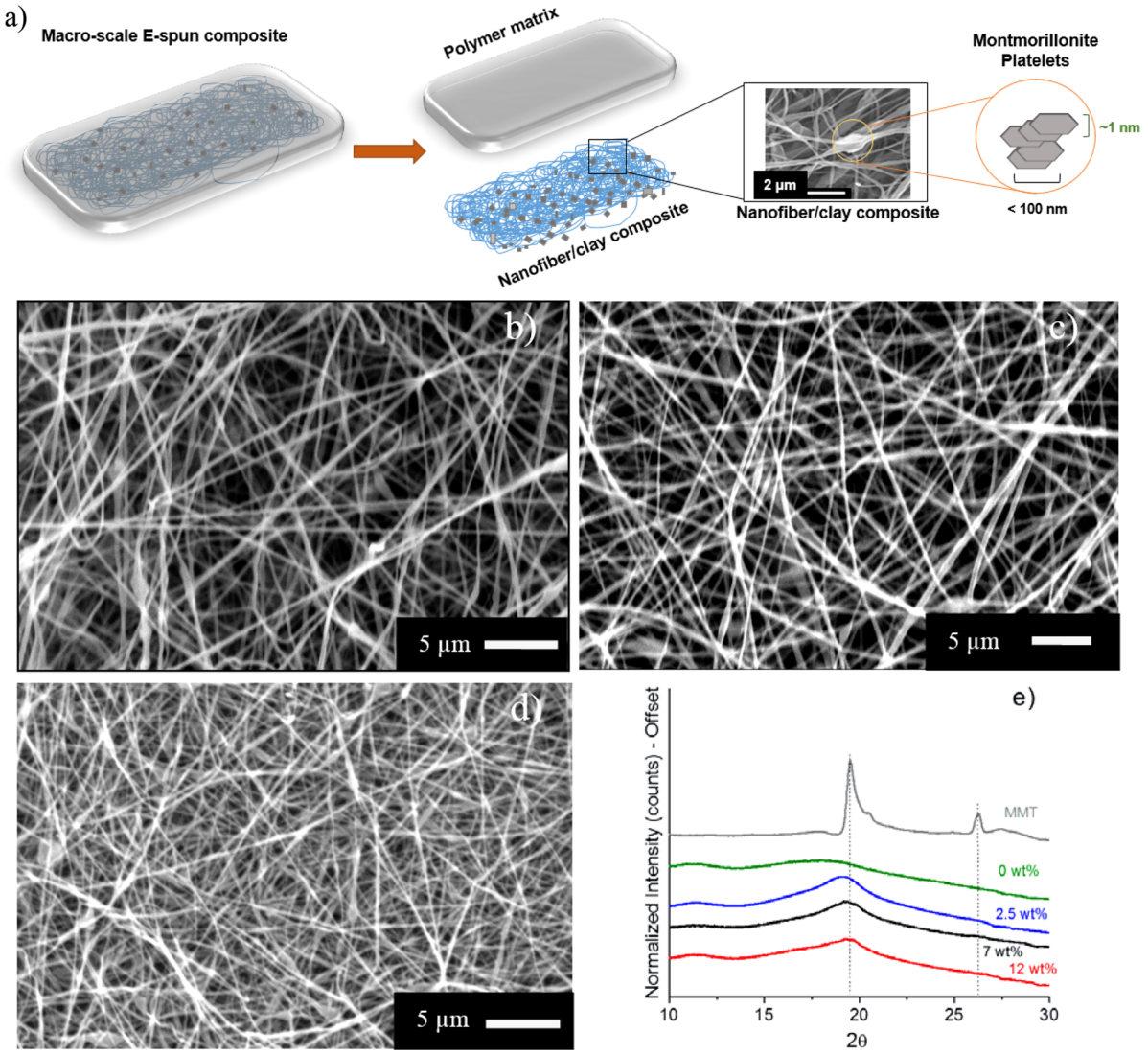

Figure 2. (a) A schematic of the hierarchical structure of the MMT-loaded electrospun composites. SEM images of electrospun mats with varying MMT weight fractions; (b) PVA/MMT 2.5, (c) PVA/MMT 7, (d) PVA/MMT 12, (e) wide-angle X-ray pattern of neat MMT and electrospun mats. Fiber diameter histograms are provided in Figure S2.

PVA−PVA bonds may not be thermodynamically favorable upon methanol treatment, resulting in lower crystallinity values. Annealing (<40 °C) or extending the soaking time in methanol may have been possible solutions to these potential barriers to crystallization of the PVA/MMT fiber fillers. However, we followed the same protocol for methanol treatment of fibers to be consistent with our previously published methodology.[20]

To further probe observed differences in crystallinity with MMT content, we also investigated the influence of the fiber diameter. Two electrospun PVA scaffolds were fabricated with different average fiber diameters of 150 ± 30 nm and 265 ± 40 nm, and DSC analysis was performed to assess the impact on crystallinity. Similar crystallinity values of 34 and 31% for 150 and 265 nm mats, respectively, were obtained. These results suggest that the effect of fiber diameter on crystallinity was minimal and that the impact of MMT filler fraction may be quite influential.

As shown in Figure 2a, the architecture of these composites was designed to exhibit two levels of hierarchy: the dispersion of MMT platelets within the fibers contribute to the first level, and the randomly oriented PVA fibers embedded within the polymeric matrix create the second level of hierarchy while maintaining an electrospun filler fraction of 4 wt % PVA/MMT fibers. Scanning electron microscopy (SEM) of fiber scaffolds revealed uniform, smooth fiber morphology (Figure 2b−d) with MMT embedded within the PVA fibers during the electrospinning process. The histograms of fiber diameter distribution indicated average fiber diameters of 275 ± 75 nm (2.5 wt %), 250 ± 100 nm (7 wt %), and 150 ± 50 nm (12 wt %). When compared to these fiber diameters, the average lateral dimensions of MMT crystallites are much smaller, in the range of 14 to 25 nm, and thus can be fully incorporated into the fibers.[32] The MMT-loaded fibers exhibited lower fiber diameters than our previously reported electrospun PVA fibers without any MMT (1052 ± 179 nm)[20] most likely due to MMT increasing solution conductivity without significantly increasing viscosity, although other mechanisms, such as decreased throughput of the spinning solution due to increased viscosity, may be in operation.[18,33] It is acknowledged that the larger fiber diameters for the previously fabricated PVA/MMT fibers may also be due to the highly variable processing conditions.[31] Wide-angle X-ray scattering of the PVA/MMT

DOI: 10.1021/acsami.5b06230
ACS Appl. Mater. Interfaces 2015, 7, 22970−22979

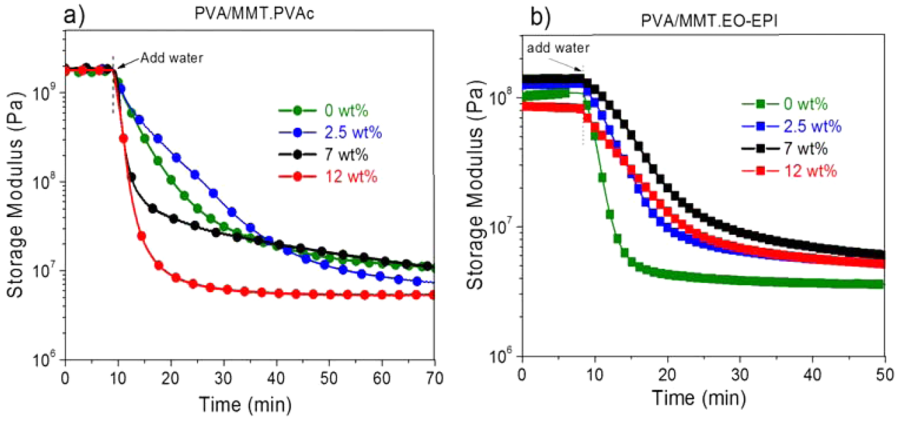

Figure 3. Hydration-induced softening of electrospun composites with varying MMT content for (a) PVAc composite and (b) EO-EPI composite.

fiber scaffolds reveals the absence of sharp MMT peaks, which hints at regions of MMT tactoids of reduced sizes.[35,36] (Figure 2e). Larger MMT tactoids would have been indicated by a reappearance of the clay spacing peak at ∼1.4 nm.[37−39] The exfoliation of MMT within the fibers is most likely the preferred dispersion to achieve the desired tunable mechanical properties in the composites. It is acknowledged that transmission electron microscopy (TEM) would have been useful to further support the MMT dispersion. However, previous studies[32] on PVA/MMT films have shown that X-ray data agreed well with the TEM results. Although these observations suggest that electrospinning allows for tuning of nanofiller dispersion in PVA/MMT fiber composites, the focus of this study was to assess the role of MMT and its interactions within the PVA fibers in modulating the water-induced mechanical response and switchability in electrospun composites.

Our recent efforts[19,20] illustrated that electrospun composite films consisting of neat PVA filler and a polymeric matrix (either EO-EPI or PVAc) exhibited the ability to alter stiffness upon hydration. The responsive mechanics upon water uptake was shown to be a function of the matrix−filler interactions and the filler crystallinity. Here, hydration was utilized to investigate the role of MMT platelets as an additional handle to tune the mechanical response. First, the swelling ratios of each of the electrospun composites were determined to assess the role of swelling on mechanical behavior. The neat PVAc film exhibited a relatively low degree of swelling of 4.1 ± 0.6% w/w.[20] The degree of swelling of PVA/MMT.PVAc composite films remained relatively constant within the error as the MMT content was increased, and composites with 2.5, 7, and 12 wt % MMT filler swelled by 18.1 ± 1.6, 19.4 ± 2.3, and 20.2 ± 2.5% w/w, respectively. These swelling ratios were relatively similar when compared to PVA.PVAc composites with no MMT (16.4 ± 3.1% w/w).[20] The similar swelling ratios may be explained by aggregation of MMT layers into smaller tactoids. In addition, the swelling data do not support clay exfoliation as exfoliated layers may provide more binding points to water.[40] The neat EO-EPI film swelled to 19.3 ± 1.9% w/w,[20] whereas PVA/MMT.EO-EPI films with 2.5, 7, and 12 wt % of MMT content swelled to 31.2 ± 1.8, 36.2 ± 3.2, and 38.1 ± 2.1% w/w, respectively. These results are statistically similar to the PVA.EO-EPI composite with no MMT content (28.3 ± 3.6% w/w),[20] suggesting that swelling behavior is relatively independent of MMT content. It is likely that the hydrophilic nature of PVA itself dominates the swelling response along with contributions from the dispersed state of the MMT.

To probe the stimuli-responsive mechanical behavior of these hierarchically designed composites upon hydration, we utilized submersion DMA to monitor the change in storage modulus of the PVA/MMT-based electrospun composites with hydration (Figure 3). The storage moduli of the MMT-containing electrospun composite films were recorded at room temperature, and deionized water was added to completely submerge the film. The EO-EPI polymer matrix exhibits a glass transition temperature (−35 °C) well below room temperature, and therefore, no complications with thermal effects of water plasticization were expected. However, PVAc is known to undergo changes in glass transition upon water plasticization of the neat PVAc matrix as indicated by the reduction of glass transition temperature to 20 °C.[33] Therefore, the experiments to investigate the hydration-induced mechanical response were specifically conducted at room temperature to avoid any contribution from the glass transition temperature range of PVAc (Figure S3). Thus, we were able to decouple the changes in stiffness due to water plasticization and temperature-induced glass transition. Adsorption and mobility of water on an MMT platelet may play roles in the switching times of the composites upon hydration. Although prior literature in this area is limited, one investigation reported high but different affinity of polymer and water molecules on the inorganic surface.[34] Their findings reveal that the density of water beads near the MMT surface is higher than that of the polymer (PEO) chains, suggesting that water molecules preferably reside on the surface of the clay, leading to higher mobility when compared to water residing between clay layers. From the DMA data for PVA/MMT.PVAc composites (Figure 3a), a general trend was observed where increasing the weight fraction of MMT resulted in a decrease in switching time. The switching time is defined as the time required for the storage modulus to decrease to a stable lower plateau modulus from a higher plateau modulus upon hydration. Thus, the composite film with the highest MMT content (12 wt %) exhibited the shortest switching time of ∼20 min, whereas switching occurred in ∼40 min for the 2.5 wt % composite, which is comparable to that of PVA.PVAc composites without any MMT content. These observations of switching time can be attributed to the highly hydrophilic nature of MMT and the interconnected MMT platelets facilitating efficient water transport. When examining the magnitude of storage modulus reduction of PVA/MMT.PVAc films upon hydration, the composite with the highest MMT

DOI: 10.1021/acsami.5b06230
ACS Appl. Mater. Interfaces 2015, 7, 22970−22979

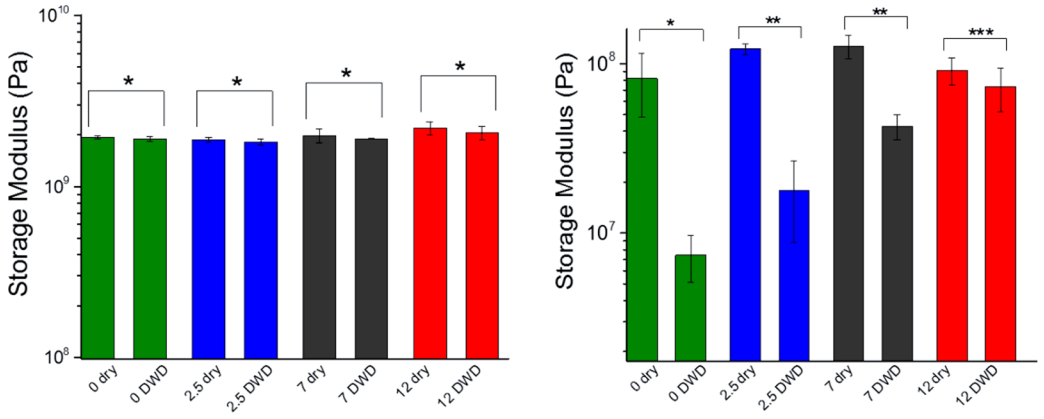

Figure 4. Storage moduli of dry and dry-wet-dry (DWD) composites at room temperature (left) PVA/MMT.PVAc (dry and DWD modulus for each weight fraction is not statistically significantly different at $*p < 0.05$), (right) PVA/MMT.EO-EPI (modulus of dry and DWD films are statistically significantly different with $*p < 0.05$, $**p < 0.01$, and for 12 wt %, dry modulus is not statistically significantly different from DWD modulus with $***p < 0.05$).

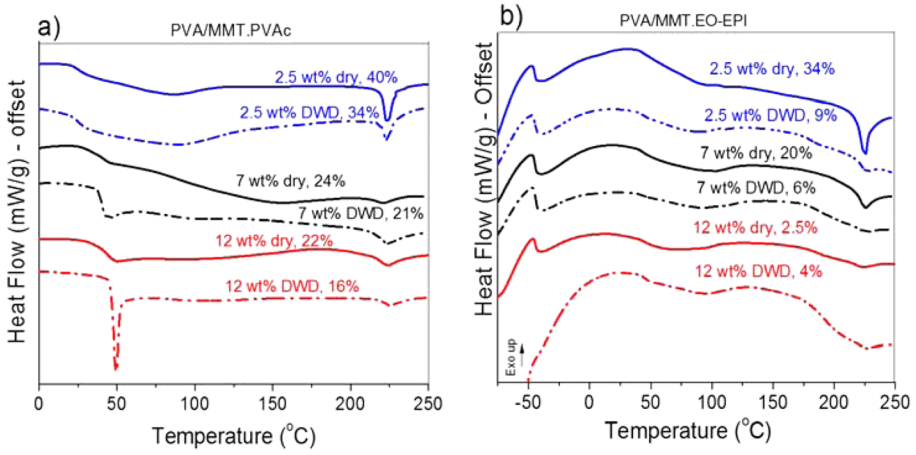

Figure 5. DSC thermograms of electrospun (a) PVA/MMT.PVAc and (b) PVA/MMT.EO-EPI composites. DWD = dry-wet-dry.

content (12 wt %) showed a significant 36-fold reduction of modulus from 2.2 GPa (dry) to 60 MPa (wet), and the film with the lowest MMT content (PVA/MMT.PVAc 2.5 wt %) showed a 16-fold storage modulus reduction from 1.9 GPa (dry) to 116 MPa (wet).

In contrast, the PVA/MMT.EO-EPI composite films typically displayed increasing switching times with an increase in weight fraction of MMT (Figure 3b). The neat EO-EPI exhibited almost instantaneous switching,[20] and the time gradually increased with an MMT weight fraction of 0 (~15 min), 2.5 (~20 min), and 7 and 12 wt % (~25 min). These slower response times of PVA/MMT.EO-EPI films were expected given that, even in the absence of MMT, strong interactions between the PVA and EO-EPI mediate a delayed, hydration-induced mechanical response of PVA.EO-EPI composites. The wet moduli (~5.5 MPa) of all EO-EPI-based films containing MMT were higher when compared to the wet modulus (2.3 MPa) of the PVA.EO-EPI film. These higher moduli in the wet state can be attributed to the inherent rigidity of MMT, which will be discussed in the section on tensile behavior. Unlike PVAc-based films, the PVA/MMT.EO-EPI films at all MMT weight fractions exhibited reductions in modulus of similar magnitude upon hydration. The storage modulus of 2.5 wt % films decreased from 122 MPa (dry) to 5.2 MPa (wet), and the modulus of 7 wt % films decreased from 126 MPa (dry) to 6.1 MPa (wet). These results related to switching times and modulus changes of PVA/MMT.EO-EPI films were quite different than those of the PVA/MMT.PVAc composites and could be attributed to competitive intermolecular interactions with water and MMT cross-bridges[41] formed between the PVA filler and EO-EPI reinforcing the MMT interface. The MMT bridges were facilitated by the strong hydrogen bonding interactions between PVA and MMT as well as ion−dipole and dipole−dipole interactions between EO-EPI and MMT. In summary, when considering the mechanical response of the PVA/MMT composites upon hydration, it can be highlighted that, in PVA/MMT.EO-EPI films, complex matrix (EO-EPI)−filler (PVA/MMT) and filler (PVA)−filler (MMT) interactions governed the water-induced switching response, whereas in PVA/MMT.PVAc films, it was the highly hydrophilic nature of MMT that dominated the reduction of modulus upon hydration.

The mechanical switchability of these water-responsive composites in the dry and dry-wet-dry states was also investigated (Figure 4). Each electrospun composite was subjected to dry-wet-dry processing, which involves soaking the films in water for 24 h and subsequent room temperature vacuum drying. Examining the mechanical behavior of PVA/MMT.PVAc composites in the dry state, only minimal modulus enhancement (e.g., no statistical difference) was observed upon

DOI: 10.1021/acsami.5b06230
ACS Appl. Mater. Interfaces 2015, 7, 22970−22979

incorporation of 2.5, 7, and 12 wt % MMT-reinforced PVA fibers, similar to the observations reported[20] previously for PVA.PVAc films without MMT. This minimal modulus enhancement was due to the relatively similar storage moduli of the filler and matrix components. Upon hydration and subsequent drying, all of the PVA/MMT.PVAc composites with 2.5, 7, and 12 wt % of MMT in PVA filler exhibited significantly restored moduli by 97, 96, and 91% to 1.8, 1.9, and 2.0 GPa, respectively (Figure 4a), similar to the two-way switchable behavior observed[19] for PVA.PVAc films without MMT. In contrast, the mechanical behavior of PVA/MMT.EO-EPI composites was quite different (Figure 4b). Examination of the PVA/MMT.EO-EPI composites in the dry state revealed that the incorporation of MMT into the PVA fibrous filler resulted in enhanced moduli of 122 ± 9 MPa (2.5 wt %), 127 ± 19 MPa (7 wt %), and 91 ± 16 MPa (12 wt %). The relatively low modulus observed for 12 wt % composites could be attributed to the reduction in PVA filler crystallinity as shown by the DSC thermograms (Figure 5). Another important observation related to PVA/MMT.EO-EPI composites was the significant restoration of storage modulus in the dry-wet-dry films, especially with higher MMT content. In contrast to the one-way switchability of EO-EPI-based dry-wet-dry composites without MMT,[20] PVA/MMT.EO-EPI dry-wet-dry composites with 7 and 12 wt % of MMT in PVA filler exhibited restored moduli of 34% to 42.7 MPa and 80% to 73.1 MPa, respectively. The composite organization remained unchanged, and delamination was not evident during the dry-wet-dry processing (Figure S1). There could be two possible reasons driving this mechanical response: (1) recrystallization of the PVA filler mediated by multicomponent interactions, and/or (2) the inherent rigidity of the percolating network of MMT platelets. These two factors were the subject of further investigation. In addition, the switchability of the composites was examined as a function of swelling ratio (Figure S4), and the results revealed significant changes in the storage moduli of EO-EPI-based composites with an increase of water uptake between dry and dry-wet-dry composites. This behavior can most likely be related to the increased hydrogen bonding capability between the hydrophilic segment of the EO-EPI and PVA/MMT after initial hydration and subsequent drying. The hydrogen bonds can be formed between the ethylene oxide segments and hydroxyl units of PVA. In contrast, the storage modulus profile of the PVAc-based system remained relatively unchanged with hydration (function of swelling ratio) and was similar to the dry-wet-dry profile, suggesting that water uptake is only a function of MMT content as supported by the swelling results. These data correlate well with the previously discussed results on water-induced modulus changes of composites, and it is evident that competitive hydrogen bonding within EO-EPI-based composites yields a delayed and less sensitive response to hydration.

To elucidate the role of filler crystallinity on responsive mechanics, we utilized DSC to probe the crystallinity of the PVA filler in the electrospun composites. The crystallinity was reproportioned by the weight of the PVA filler fraction in the composite. For PVA/MMT.PVAc films below the MMT percolation threshold, the PVA/MMT.PVAc composite film containing 2.5 wt % of MMT in PVA exhibited the highest crystallinity (40%) in the dry state (Figure 5a) and recrystallization after dry-wet-dry processing, resulting in full restoration of storage moduli. When the MMT loading was increased beyond the percolation threshold, the crystallinity of PVA within the PVA/MMT composites decreased to 24 and 22% for 7 and 12 wt % systems, respectively. However, these composite films exhibited significant recrystallization after dry-wet-dry processing, contributing to the restored storage moduli. In contrast, the PVA/MMT.EO-EPI composite films exhibited unusual recrystallization behavior of PVA upon dry-wet-dry processing compared to that of PVA.EO-EPI composites. The incorporation of 2.5 wt % of MMT into PVA resulted in only 9% recrystallization of the PVA filler in the composite films after dry-wet-dry processing, and the percent recrystallization continued to decrease above the MMT percolation threshold (Figure 5b). As has been suggested in the polymer/clay literature,[42] this recrystallization of PVA is mainly attributed to the surface-induced crystallization near the PVA/MMT interfaces instead of the PVA-rich zones away from the MMT platelets. The DSC results suggest that crystallinity may have played only a minimal role in the observed restored moduli in these hierarchical PVA/MMT.EO-EPI composites; however, it does not fully explain why the lowest recrystallization value of 12 wt % dry-wet-dry EO-EPI-based composites results in the highest restored storage modulus. Therefore, we chose to explore the effects of inherent rigidity and stiffness of the MMT platelets on the restored modulus of the PVA/MMT.EO-EPI composites after dry-wet-dry processing.

To investigate the relationship between the observed switchability and the rigidity or stiffness of MMT, we fabricated PVA/MMT electrospun mats, and tensile testing was performed prior to the methanol treatment (Figure 6).

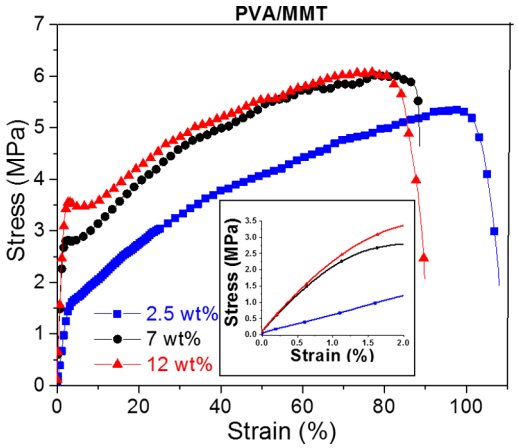

Figure 6. Typical stress–strain diagrams of electrospun PVA/MMT mats. Figure inset shows a magnified image of the initial region of the curves.

As shown previously in Figure 1, the similar crystallinity values of PVA mats prior to methanol-soak provided an opportunity to examine the effects of rigidity of MMT. The stress–strain tests were performed on as-spun PVA/MMT mats to determine the Young's modulus (1% secant modulus), tensile strength, and strain-at-break. The Young's modulus (corrected for 86% porosity) increased with increasing MMT fraction, and a significant 3-fold increase from 11.9 to 30.4 MPa was observed for mats of 2.5 and 7 wt %, respectively (Table 1). For 12 wt % films, the Young's modulus continued to increase to ~34.3 MPa, whereas the strain-at-break decreased to ~72.4%. This increase in modulus for 7 and 12 wt % PVA/MMT mats may be attributed to the MMT fraction exceeding the percolation threshold, suggesting a key hierarchical

DOI: 10.1021/acsami.5b06230
ACS Appl. Mater. Interfaces 2015, 7, 22970–22979

Table 1. Mechanical Properties of PVA/MMT Mats[a]

MMT %	elastic modulus (MPa)	strain-at-break (%)
0	9.9 ± 1.7	150 ± 29.2
2.5	11.9 ± 2.1	106.9 ± 14.9
7	30.4 ± 3.2*	82.6 ± 25.4**
12	34.3 ± 5.8*	72.4 ± 17.2***

[a]Statistically significantly different from 2.5 wt % at *$p < 0.05$ and ***$p < 0.1$; statistically not significantly different from 2.5 wt % with **$p < 0.05$. A porosity of 86% was considered in calculating modulus values.

connection between MMT content, percolation, and mechanical behavior. The enhancement effect of the PVA/MMT electrospun nanofibers is further examined utilizing a percolation model.[37] This model considers a percolated network of nanofillers reinforcing the polymer matrix, in this case PVA, and includes consideration of orientation and porosity. Details of the calculations are provided in the Supporting Information. The theoretical elastic moduli obtained by the percolation model were 18.2 and 44.7 MPa for 7 and 12 wt % PVA/MMT mats, respectively. These values agree closely with the experimental moduli when porosity was considered, which supports the idea of a percolated network of MMT within the fibers. However, these theoretical calculations do not provide definitive evidence necessary to exclude the impact of tactoids formed within the percolated network structure. Overall, these results strongly suggest that inherent rigidity coupled with the MMT dispersion significantly impact the mechanical behavior of the electrospun PVA mats. This behavior is quite apparent in the enhanced storage modulus of PVA/MMT.EO-EPI 12 wt % films in the absence of significant recrystallization; at these higher weight fractions, this mechanical response suggests that rigidity and non-uniform MMT dispersion play an important role in increasing the dry-wet-dry modulus. Overall, these results suggest that it is the synergistic interplay between PVA crystallinity, hydration pathways, MMT reinforcement, and organization within the PVA/MMT filler that influences the responsive behavior of these hierarchical electrospun composites.

4. CONCLUSIONS

We have explored the effects of nanoclay reinforcement as it relates to tuning of the mechanical properties of hierarchical electrospun composites. Hydration was utilized to investigate the role of clay as an additional handle to tune the mechanical response. An electrospun mat of PVA containing different weight fractions of MMT was incorporated into either a rubbery or glassy polymeric matrix of EO-EPI or PVAc, respectively. MMT dispersion within the fibers may have a significant impact on the switchable mechanics. WAXS spectra revealed an absence of characteristic MMT peaks, suggesting either exfoliation or smaller tactoid formation. Swelling experiments and theoretical calculations of percolation of MMT within the PVA fibers suggest percolation with the possibility of smaller tactoid formation. The incorporation of MMT into the PVA fibrous filler resulted in enhanced moduli for PVA/MMT.EO-EPI composites in the dry state due to the reinforcing effect of the higher modulus electrospun mat. However, MMT-loaded PVA fibers did not significantly enhance the storage moduli of PVA/MMT.PVAc films at room temperature, which was attributed to the relatively similar storage moduli of the PVAc matrix and PVA/MMT electrospun mat.

The mechanical response upon hydration was highly dependent on the weight-fraction of MMT in the PVA fibers. A general trend was observed in PVA/MMT.PVAc composites where increasing the weight fraction of MMT resulted in a decrease in switching time due to the highly hydrophilic nature of the MMT platelets and their interconnected structure facilitating efficient water transport. In contrast, PVA/MMT.EO-EPI composite films exhibited a general trend of increasing switching times with an increase in weight fraction of MMT compared to almost instantaneous switching in neat EO-EPI. This dynamic mechanical response upon water uptake could be attributed to competitive intermolecular interactions with water and MMT cross-bridges[26] formed between the PVA filler and EO-EPI reinforcing the MMT interface. PVA/MMT.PVAc films exhibited substantial recrystallization of PVA after dry-wet-dry processing, contributing to the restored storage moduli and two-way switchability. The influence of MMT may be an interesting parameter for future investigations because the inherent rigidity and dispersion of MMT will play a major role in restoring the mechanical properties. The lower percolation threshold obtained for higher aspect ratios will certainly reduce the impact on crystallinity. Although PVA/MMT.EO-EPI composites with 2.5 and 7 wt % MMT exhibited only partial restoration of modulus after dry-wet-dry processing, the 12 wt % PVA/MMT.EO-EPI dry-wet-dry film did exhibit significant restoration of storage modulus upon hydration and subsequent drying. It was revealed that the observed mechanical behavior observed in these PVA/MMT.EO-EPI electrospun composites is a complex function of MMT rigidity, PVA crystallinity, and hydration-induced interfacial interactions between MMT, PVA, and the EO-EPI matrix.

In this work, we have designed functional and adaptable composites utilizing the concepts of hierarchy and percolation and determined that the unique interplay between crystallinity, MMT content, and matrix−filler interactions can be engineered to control the mechanical response. Coupled with an easy and straightforward fabrication method, this composite technology is highly attractive in applications ranging from sensor platforms to transdermal drug delivery vehicles.

■ ASSOCIATED CONTENT

Supporting Information

The Supporting Information is available free of charge on the ACS Publications website at DOI: 10.1021/acsami.5b06230.

Composite and fiber mat analysis via SEM of the cross-sectional area and fiber diameter histograms, DMA of the PVAc matrix, swelling behavior for both EO-EPI and PVAc matrices, and analysis of MMT percolation within the PVA electrospun fibers (PDF)

■ AUTHOR INFORMATION

Corresponding Author

*E-mail: lashanda.korley@case.edu.

Funding

The authors acknowledge financial support from the 3M Nontenured Faculty Grant and the National Science Foundation (CAREER DMR-0953236).

Notes

The authors declare no competing financial interest.

DOI: 10.1021/acsami.5b06230
ACS Appl. Mater. Interfaces 2015, 7, 22970−22979

■ ACKNOWLEDGMENTS

The authors acknowledge the Center for Layered Polymeric Systems (CLiPS) for use of their SEM.

■ ABBREVIATIONS

DWD, dry-wet-dry; MMT, montmorillonite; EO-EPI, ethylene oxide−epichlorohydrin copolymer; PVA, poly(vinyl alcohol); PVAc, poly(vinyl acetate); CEC, cation exchange capacity; MW, molecular weight

■ REFERENCES

(1) Tai, K.; Dao, M.; Suresh, S.; Palazoglu, A.; Ortiz, C. Nanoscale Heterogeneity Promotes Energy Dissipation in Bone. *Nat. Mater.* **2007**, *6*, 454−462.
(2) Gupta, H. S.; Seto, J.; Wagermaier, W.; Zaslansky, P.; Boesecke, P.; Fratzl, P. Cooperative Deformation of Mineral and Collagen in Bone at the Nanoscale. *Proc. Natl. Acad. Sci. U. S. A.* **2006**, *103*, 17741−17746.
(3) Stone, A. D.; Korley, L. T. J. Bioinspired Polymeric Nanocomposites. *Macromolecules* **2010**, *43*, 9217−9226.
(4) Wanasekara, N. D.; Korley, L. T. J. Toward Tunable and Adaptable Polymer Nanocomposites. *J. Polym. Sci., Part B: Polym. Phys.* **2013**, *51*, 463−467.
(5) Ramesh, S.; Sivasamy, A.; Alagar, M.; Chandrasekar, F. Synthesis and Characterization of poly(n-vinyl-2-pyrrolidone)-organo-modified Montmorillonite (OMMT) Clay Hybrid Nanocomposites. *J. Compos. Mater.* **2011**, *45*, 1483−1489.
(6) Valandro, S. R.; Lombardo, P. C.; Poli, A. L.; Horn, M. A., Jr.; Neumann, M. G.; Cristina, C.; Cavalheiro, S. Thermal Properties of Poly (Methyl Methacrylate)/Organomodified Montmorillonite Nanocomposites Obtained by in situ Photopolymerization. *Mater. Res.* **2013**, *17*, 265−270.
(7) Vaia, R. A.; Giannelis, E. P. Lattice Model of Polymer Melt Intercalation in Organically-Modified Layered Silicates. *Macromolecules* **1997**, *30*, 7990−7999.
(8) Lee, B. P.; Messersmith, P. B.; Israelachvili, J. N.; Waite, J. H. Mussel-Inspired Adhesives and Coatings. *Annu. Rev. Mater. Res.* **2011**, *41*, 99−132.
(9) Gilman, J. Flammability and Thermal Stability Studies of Polymer Layered-Silicate (clay) Nanocomposites. *Appl. Clay Sci.* **1999**, *15*, 31−49.
(10) Kojima, Y.; Usuki, A.; Kawasumi, M.; Okada, A.; Fukushima, Y. Mechanical Properties of Nylon 6-clay Hybrid. *J. Mater. Res.* **1993**, *8*, 1185−1189.
(11) James Korley, L. T.; Liff, S. M.; Kumar, N.; McKinley, G. H.; Hammond, P. T. Preferential Association of Segment Blocks in Polyurethane Nanocomposites. *Macromolecules* **2006**, *39*, 7030−7036.
(12) Liff, S. M.; Kumar, N.; McKinley, G. H. High-performance Elastomeric Nanocomposites via Solvent-exchange Processing. *Nat. Mater.* **2007**, *6*, 76−83.
(13) Neppalli, R.; Wanjale, S.; Birajdar, M.; Causin, V. The effect of clay and of electrospinning on the polymorphism, structure and morphology of poly(vinylidene fluoride). *Eur. Polym. J.* **2013**, *49*, 90−99.
(14) Bergshoef, M. M.; Vancso, G. J. Transparent Nanocomposites with Ultrathin, Electrospun Nylon-4,6 Fiber Reinforcement. *Adv. Mater.* **1999**, *11*, 1362−1365.
(15) Kim, J.; Reneker, D. H. Mechanical Properties of Composites Using Ultrafine Electrospun Fibers. *Polym. Compos.* **1999**, *20*, 124−131.
(16) Choi, J.; Lee, K. M.; Wycisk, R.; Pintauro, P. N.; Mather, P. T. Nanofiber Network Ion-Exchange Membranes. *Macromolecules* **2008**, *41*, 4569−4572.
(17) Neppalli, R.; Marega, C.; Marigo, A.; Bajgai, M. P.; Kim, H. Y.; Causin, V. Poly(e-caprolactone) filled with electrospun nylon fibres: A model for a facile composite fabrication. *Eur. Polym. J.* **2010**, *46*, 968−976.
(18) Neppalli, R.; Causin, V.; Marega, C.; Saini, R.; Mba, M.; Marigo, A. Structure, Morphology, and Biodegradability of Poly(e-caprolactone)-Based Nanocomposites. *Polym. Eng. Sci.* **2011**, *51*, 1489−1496.
(19) Stone, D. A.; Wanasekara, N. D.; Jones, D. H.; Wheeler, N. R.; Wilusz, E.; Zukas, W.; Wnek, G. E.; Korley, L. T. J. All-Organic, Stimuli-Responsive Polymer Composites with Electrospun Fiber Fillers. *ACS Macro Lett.* **2012**, *1*, 80−83.
(20) Wanasekara, N. D.; Stone, D. A.; Wnek, G. E.; Korley, L. T. J. Stimuli-Responsive and Mechanically-Switchable Electrospun Composites. *Macromolecules* **2012**, *45*, 9092−9099.
(21) Yao, L.; Haas, T. W.; Guiseppi-elie, A.; Bowlin, G. L.; Simpson, D. G.; Wnek, G. E. Electrospinning and Stabilization of Fully Hydrolyzed Poly(Vinyl Alcohol) Fibers. *Chem. Mater.* **2003**, *15*, 1860−1864.
(22) Korley, L. T. J.; Wnek, G. E.; Stone, D. A.; Wanasekara, N. D. Electrospun Mats as Fillers for Polymer Nanocomposites with Applications in Stimuli-Responsive Mechanics, Drug Delivery & Optical Modulation. US Patent Appl. 2012171040, 2012.
(23) Strawhecker, K. E.; Manias, E. AFM of Poly(vinyl alcohol) Crystals Next to an Inorganic Surface. *Macromolecules* **2001**, *107*, 8475−8482.
(24) Kim, D. Preparation and Characterization of Crosslinked PVA/SiO2 Hybrid Membranes Containing Sulfonic Acid Groups for Direct Methanol Fuel Cell Applications. *J. Membr. Sci.* **2004**, *240*, 37−48.
(25) Son, J.; Kang, Y.; Won, J. Poly(vinyl alcohol)-based Polymer Electrolyte Membranes Containing Polyrotaxane. *J. Membr. Sci.* **2006**, *281*, 345−350.
(26) Kim, T. K.; Kang, M.; Choi, Y. S.; Kim, H. K.; Lee, W.; Chang, H.; Seung, D. Preparation of Nafion-sulfonated Clay Nanocomposite Membrane for Direct Menthol Fuel Cells via a Film Coating Process. *J. Power Sources* **2007**, *165*, 1−8.
(27) Yang, C. C.; Lee, Y. J. Preparation of the Acidic PVA/MMT Nanocomposite Polymer Membrane for the Direct Methanol Fuel Cell (DMFC). *Thin Solid Films* **2009**, *517*, 4735−4740.
(28) Fredrickson, G. H.; Bicerano, J. Barrier Properties of Oriented Disk Composites. *J. Chem. Phys.* **1999**, *110*, 2181−2188.
(29) Lee, J.; Bhattacharyya, D.; Easteal, A. J.; Metson, J. B. Properties of nano-ZnO/poly(vinyl alcohol)/poly(ethylene oxide) composite thin films. *Curr. Appl. Phys.* **2008**, *8*, 42−47.
(30) Gao, H.; Lian, K. Advanced proton conducting membrane for ultra-high rate solid flexible electrochemical capacitors. *J. Mater. Chem.* **2012**, *22*, 21272−21278.
(31) Sengwa, R. J.; Choudhary, S.; Sankhla, S. Dielectric Properties of Montmorillonite Clay Filled Poly(vinyl alcohol)/Poly(ethylene oxide) Blend Nanocomposites. *Compos. Sci. Technol.* **2010**, *70*, 1621−1627.
(32) Jonas, E. C.; Oliver, R. T. M. Size and Shape of Montmorillonite Crystallites Clays. *Clays Clay Miner.* **1967**, *15*, 27−33.
(33) Rubin, D. J.; Nia, H. T.; Desire, T.; Nguyen, P. Q.; Gevelber, M.; Ortiz, C.; Joshi, N. S. Mechanical Reinforcement of Polymeric Fibers through Peptide Nanotube Incorporation. *Biomacromolecules* **2013**, *14*, 3370−3375.
(34) Toth, R.; Voorn, D.-J.; Handgraaf, J.-W.; Fraaije, J. G. E. M.; Fermeglia, M.; Pricl, S.; Posocco, P. Multiscale Computer Simulation Studies of Water-Based Montmorillonite/Poly(ethylene oxide) Nanocomposites. *Macromolecules* **2009**, *42*, 8260−8270.
(35) Soon, K.; Harkin-Jones, E.; Rajeev, R. S.; Menary, G.; Martin, P. J.; Armstrong, C. G. Morphology, Barrier, and Mechanical Properties of Biaxially Deformed Poly(ethylene terephthalate)-Mica Nanocomposites. *Polym. Eng. Sci.* **2012**, *52*, 532−548.
(36) Todorov, L. V.; Martins, C. I.; Viana, J. C. In Situ WAXS/SAXS Structural Evolution Study During Uniaxial Stretching of Poly(ethylene therephthalate) Nanocomposites in Solid State: Poly(ethylene therephthalate)/Montmorillonite Nanocomposites. *J. Appl. Polym. Sci.* **2013**, *128*, 2884−2895.
(37) Capadona, J. R.; Shanmuganathan, K.; Tyler, D. J.; Rowan, S. J.; Weder, C. Stimuli-responsive Polymer Nanocomposites Inspired by the Sea Cucumber Dermis. *Science* **2008**, *319*, 1370−1374.

DOI: 10.1021/acsami.5b06230
ACS Appl. Mater. Interfaces 2015, 7, 22970−22979

(38) Bandi, S.; Schiraldi, D. A. Glass Transition Behavior of Clay Aerogel/Poly(vinyl alcohol) Composites. *Macromolecules* **2006**, *39*, 6537−6545.
(39) Mondal, D.; Mollick, Md. M. R.; Bhowmick, B.; Maity, D.; Bain, M. K.; Rana, D.; Mukhopadhyay, A.; Dana, K.; Chattopadhyay, D. Effect of poly(vinyl pyrrolidone) on the morphology and physical properties of poly(vinyl alcohol)/sodium montmorillonite nanocomposite films. *Prog. Nat. Sci.* **2013**, *23*, 579−587.
(40) Chen, P.; Zhang, L. Interaction and Properties of Highly Exfoliated Soy Protein/Montmorillonite Nanocomposites. *Biomacromolecules* **2006**, *7*, 1700−1706.
(41) Lee, H. W.; Karim, M. R.; Ji, H. M.; Choi, J. H.; Ghim, H. D.; Park, S. M.; Oh, W.; Yeum, J. H. Electrospinning Fabrication and Characterization of Poly(vinyl alcohol)/ Montmorillonite Nanofiber Mats. *J. Appl. Polym. Sci.* **2009**, *113*, 1860−1867.
(42) Strawhecker, K. E.; Manias, E. Structure and Properties of Poly(vinyl alcohol)/Na+ Montmorillonite Nanocomposites. *Chem. Mater.* **2000**, *12*, 2943−2949.

DOI: 10.1021/acsami.5b06230
ACS Appl. Mater. Interfaces 2015, 7, 22970−22979